Synthesis and Photoelectrocatalytic Performance of Mn-N-TiO₂/Ti Electrode for Electrochemical Sensor

L O Mursalim A M[1], Ruslan[2], R A Safitri[1], T Azis[1], Maulidiyah[1], D Wibowo[1], M Nurdin*[1]

[1]Department of Chemistry, Faculty of Mathematics and Natural Sciences, Universitas Halu Oleo, Jl. H.E.A. Mokodompit, Kendari 93232 – Southeast Sulawesi, Indonesia.
[2]Department of Chemistry, Faculty of Mathematics and Natural Sciences, Univesitas Tadulako, Jl. Soekarno-Hatta, Palu 94118 – Central Sulawesi, Indonesia

E-mail: *[1] mnurdin06@yahoo.com

Abstract. Preparation of manganese (Mn) and nitrogen (N)-doped TiO_2/Ti electrode as a COD sensor was successfully performed to enhance photoelectrocatalytic activity under visible light. The preparation of Mn and N using the sol-gel method then coated on TiO_2 thin layer hidrothermal by dip-coating technique. Characterization of Mn-N-TiO_2/Ti electrode using FTIR showed that indicated the Ti-O, Ti-N, N-O, and Mn-O bonds. SEM-EDX showed a thin layer formed of Mn and N on TiO_2/Ti surface with the Mn, N, Ti, O spectrums at 0.277 KeV, 0.677 KeV, 4.508 KeV, and 0.579 KeV, respectively. The photoelectrochemical test using a potentiostat was indicated that Mn-N-TiO_2/Ti electrode active under visible light which evidenced by photocurrent response.

1. Introduction

Titanium dioxide (TiO_2) is a semiconductor material widely used for photocatalysis, microelectronics, optical cells, inactivation of microorganisms, anti-fogging and self-cleaning [1,2]. TiO_2 phase in anatase crystal was the most effective form and widely used as a photocatalyst because it has high chemical and physical stability, non-toxic, low-cost, and higher photoactivity compared to other semiconductor types [3,4]. The disadvantage of TiO_2 was it could only activated by UV light irradiation with a band gap energy (Eg) of 3.2 eV [5,6]. The limitations of TiO_2 photoactivity can be overcome to modified TiO_2 material by using inserted element (dopants) to activate it under visible light [7,8].

The doping method is one of TiO_2 modification techniques performed by adding another dopant into TiO_2 crystal lattice. Modification of TiO_2 has developed to increase TiO_2 activity in visible light and separate it from electrons and holes [9]. The common non-metallic dopants which generally added to TiO_2 are Nitrogen (N) [10], Sulfur (S) [11], Phosphorus (P) [12], Carbon [13] and Fluor (F) [14]. According to Yin et al. a variety of non-metallic elements as dopants which showed N dopant is effective to lowers TiO_2 band gap energy [15]. This phenomenon was increased TiO_2 thin film activity in visible light. The efficiency of photocatalysts with single N-TiO_2 dopant under visible light irradiation is still very limited [16].

In the last few decades, transition metal dopants were studied to increase the TiO_2 photocatalysis activity, such as Fe [17,18], Co [19], Ni [20], Cu [4], and Mn [21]. Manganese (Mn) is one of transition metals which has electropositive charge and has excellent electrical conductivity properties [22], it was potentially use as metal ion dopant [23]. Choudhury et al. have tested TiO_2 photocatalyst activity by Mn metal ions doped under visible light shows better results compared to TiO_2 without doping of Mn metal ions [24]. Hu et al. and Zhao et al. succeeded in synthesizing Mn and N-doped TiO_2 (Mn-N-TiO_2) using a sol-gel method which can decrease the energy gap and show strong wavelength absorption at 400 ~ 650 nm in photocatalysts performance [25,26]. Mn and N dopants also improve thermal stability in TiO_2 structure and high-photocatalytic activity to degrade organic dyes.

High-photocatalytic activity of Mn-N-TiO_2 catalysts could not apply to degrade organic dyes. Therefore, it is necessary for high ordered Mn-N-TiO_2 application to determine the Chemical Oxygen Demand (COD) sensor by photoelectrocatalysis [27,28]. The approach to the photoelectrochemical transfer by Faraday Law $(Q = nVFC)$ as photocurrent response was proportional to increase the concentration organic dyes. Nurdin et al. has developed a photoelectrocatalysis based on a COD sensor system with TiO_2/Ti working as electrode on Indium Tin Oxide (ITO) conductive glass giving it a high-performance in determining COD values [29]. Based on literatures, TiO_2 modification by metal and non-metallic dopants to develop COD sensors is still rarely explored. In this study, we have synthesized Mn-N-TiO_2 to develop the photoelectrocatalyst electrochemical sensor.

2. Experimental

2.1. Preparation of Titanium (Ti) foil

Preparation of Ti plate was performed by cutting Ti plate with purity of 99.7% and 0.5 mm thickness to size of 4 cm × 0.5 cm. It was sanded with 1200CC fine sandpaper until the surface was clean, shiny, and washed with the detergent solution, water and distilled water (D.I. H_2O). The foil was etched in HF, HNO_3, and D.I. H_2O in ratio 1:3:6 for two minutes. All chemicals were used to remove fat and oxide layer on Ti foil. The final stage was to rinse Ti foil with D.I. H_2O in order to remove residual etching solution on the surface [30].

2.2. Fabrication of TiO_2 hydrothermal electrode

A highly ordered TiO_2 electrode was synthesized by hydrothermal method. The oxidation process Ti foil was carried out in saucer porcelain and added by D.I. H_2O until it is well immersed. Then it is annealing at the temperature of 500°C to oxidation process by D.I. H_2O-assisted to form the TiO_2 in anatase structure.

2.3. Preparation of Mn-N-TiO_2/Ti by Sol-gel method

Aqueous TiO_2 colloid was prepared by the hydrolysis of titanium tetra-isopropoxide (TTIP) according to the method described by Maulidiyah et al [8]. Sol-gel was prepared by adding the 30 mL ethanol, 2 mL D.I. H_2O, 4 mL TTIP, 0.5 mL acetylacetonate (AcAc), and 1 mL acetic acid (0.5M). The solution was mixed and refluxed for 3 hours at temperature 50°C and stirred using a magnetic stirrer. After 1 hour followed by adding of 2 mL $CO(NH_2)_2$ 0.5 M and 1 mL $MnCl_2.4H_2O$ 2.5% solution to obtain the sol-gel N and Mn. The resulting sol was evaporated at room temperature for 48 hours to form a gel. Furthermore, the gel was heated in the oven at temperature 80°C for 30 minutes. The coating process was done by dip-coating technique on the TiO_2/Ti areas than calcined for 15 minutes at temperature of 150°C.
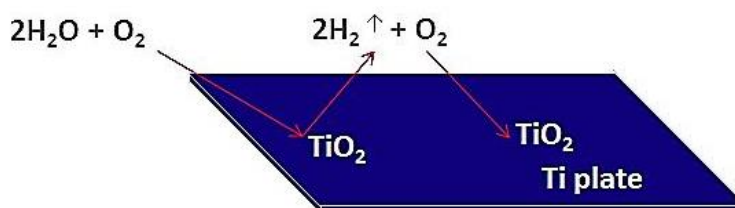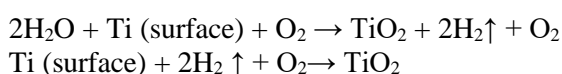
2.4. Photocurrent response in Electrochemical

Photocurrent response test was done by using Mn-N-TiO$_2$ electrode as working electrode, Pt as a counter electrode, and Ag/AgCl as a reference electrode were carried out in 0.1M NaNO$_3$ as electrolyte solution by Multi-Pulse Amperometry (MPA) I-t with bias potential 0.5 V, run-time 60 s under visible light irradiation.

3. Results and Discussion

3.1. Synthesis of TiO$_2$ thin film by hydrothermal method

Hydrothermal oxidation is a synthesis of TiO$_2$ thin film, which usually used by using D.I. H$_2$O at high temperature. Ti foil was prepared then annealed in 500°C to vapour the H$_2$O in order to remove residual solution. The annealing aimed to grow the TiO$_2$ by oxidation reaction from H$_2$O and roasting (O$_2$) process, where the mechanism can be seen in Figure 1:

$$2H_2O + Ti \text{ (surface)} + O_2 \rightarrow TiO_2 + 2H_2\uparrow + O_2$$
$$Ti \text{ (surface)} + 2H_2 \uparrow + O_2 \rightarrow TiO_2$$

Figure 1. Schematic mechanism reaction on Ti foil by hydrothermal method

The remaining O$_2$ in the hydrothermal system serves to increase the amount of oxygen to accelerate Ti metal oxidation process [22]. Nurdin et al. have reported that the observed anatase crystalline form occurring on heating TiO$_2$ at temperature of 120°C could reach its perfect temperature at 500°C [31]. The long process of sintering need to be considered as it could affect the formed crystal phase. At the same temperature with different sintering times, it will produce different crystal phases. This research conducted sintering process at 500°C temperatures for 90 minutes to produce an anatase crystalline structure which has high-photocatalyst activity compared to other crystal structures [32,33]. The profile of the obtained TiO$_2$/Ti hydrothermal electrode can be seen in Figure 2.

Figure 2. TiO$_2$ thin film hydrothermal on Ti foil

The Ti plate surface has been grown by TiO$_2$ underwent a color change to purplish blue. According to Xiong et al. the color change of titanium metal shows the formation of TiO$_2$ oxide crystals on the surface and the probability of Ti^{3+} ion concentration in TiO$_2$ crystals to provide characteristics in the visible light spectrum [33].

3.2. TiO$_2$/Ti hydrothermal doped Manganese (Mn) and Nitrogen (N)

The coating of TiO$_2$/Ti thin film with Mn and N was performed by sol-gel method. The sol-gel method has advantages compared to other techniques for thin film deposition, i.e. it is excellent in composition control and to produce high-surface area on TiO$_2$ thin film substrate [10]. The precursors in sol-gel which used in this study was TTIP as a medium for distributing dopant ions to form Mn-N-TiO$_2$/Ti,

AcAc as a stabilizer and inhibit hydrolyzed TTIP when reacted with D.I. H_2O and ethanol. Precursors of TTIP, AcAc, ethanol, acetic acid and D.I. H_2O were refluxed for three hours at 50°C to increase the interaction of the compounds [34]. The addition of acetic acid was carried out to control the hydrolysis rate and assist the pore formation process to the TiO_2 mesoporous of anatase phase [10].

The addition of $MnCl_2.4H_2O$ as the Mn source and $CO(NH_2)_2$ as the N source have been done previously by Zhao et al. TiO_2/Ti hydrothermal electrode was coated with Mn and N sol-gel by dip-coating technique, then the electrode was sintered at 150°C [26,35]. This condition aimed to attach Mn-N-TiO_2 thin layer will be stronger bonds, to remove the water solvent and can form TiO_2 crystals of anatase phase [36]. TiO_2/Ti hydrothermal electrode which was doped by Mn and N can be seen in Figure 3.
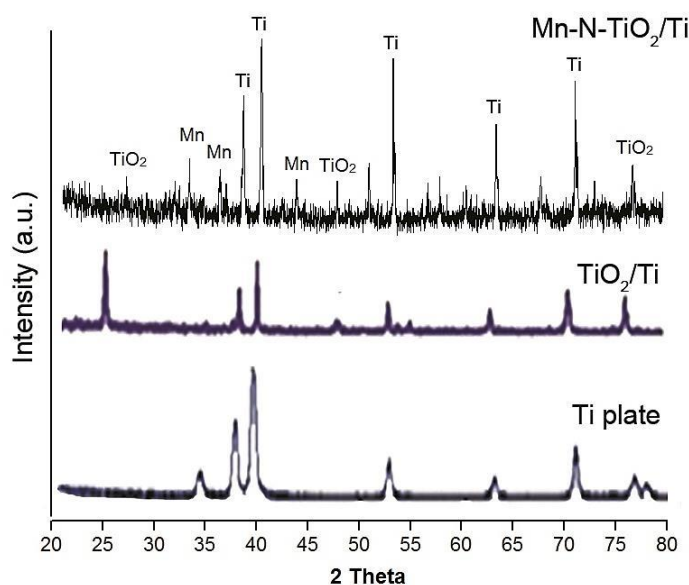

Figure 3. The Mn-N-TiO_2/Ti electrode

3.3. Characterization of Mn-N-TiO_2/Ti electrode

3.3.1. X-Ray Diffraction (XRD)

Characterization by XRD has carried out to investigate the composition, phase structure, and crystalline of the as-synthesized sample. The material type has determined by comparing XRD characterization data with the synthesized Mn-N-TiO_2/Ti pattern. Figure 4 shows diffraction pattern of Mn-N-TiO_2/Ti hydrothermal electrode.


Figure 4. XRD patterns of Mn-N-TiO_2/Ti electrode compared to reference [31]

The XRD diffractogram of Mn-N-TiO_2/Ti electrode shows the specific peaks has been identified MnO_2, TiO_2, and Ti metal crystals. The Mn-N-TiO_2/Ti hydrothermal electrode from synthesis results is a rutile crystal type at 2 theta of 27°. The formation of rutile crystals is caused by inserting Mn atoms in TiO_2 matrix, thus changing the TiO_2 anatase phase in crystal structure. MnO_2 crystals formed on TiO_2 by sol-gel method at 2 theta of 32°, 37°, and 44° [37].

Mn and TiO_2 peaks appearing on XRD data indicate Mn and N sol-gel are well attached to TiO_2/Ti hydrothermal surface.

3.3.2. Energy Dispersive X-ray (EDX)

Characterization performed by using EDX on electrode surface to determine the presence of Mn and N elements. The results of EDX characterization on Mn-N-TiO_2/Ti electrode surface can be seen in Figure 5.
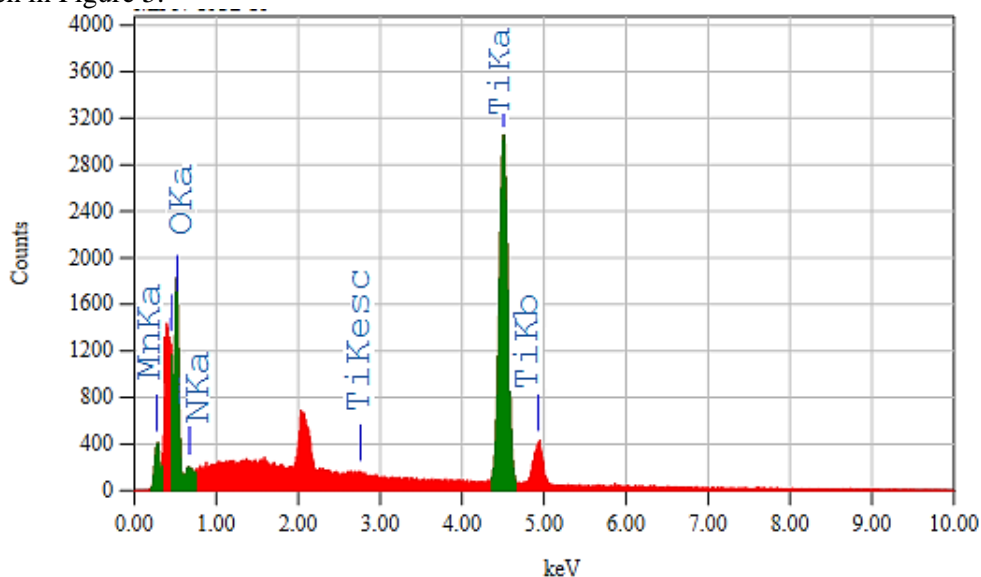

Figure 5. EDX spectra analyst of Mn-N-TiO_2/Ti electrode

EDX spectra showed the Mn peaks at 0.277 KeV, N at 0.677 KeV, Ti at 4.508 KeV and O at 0.579 KeV with the composition amount of 2.05 w%; 2.55 w%; 58.38 w%, and 37.02 w%, respectively. The calculated empirical formula from EDX data is the formation $Mn_1N_{0.3}Ti_{24.8}O_5$. The high Ti value existed from Ti plate substrate giving the highest intensity. The peaks of Mn and N indicate the presence of Mn and N which shows the success of Mn metal and N non-metal dopings by dip-coating technique.

3.3.3. Fourier Fransform Infra-Red (FTIR)

Characterization with FTIR was performed to obtain the structure of a molecule especially the functional groups seen in specific areas. The characterization result of Mn-N-TiO_2/Ti electrode with FTIR can be seen in Figure 6.
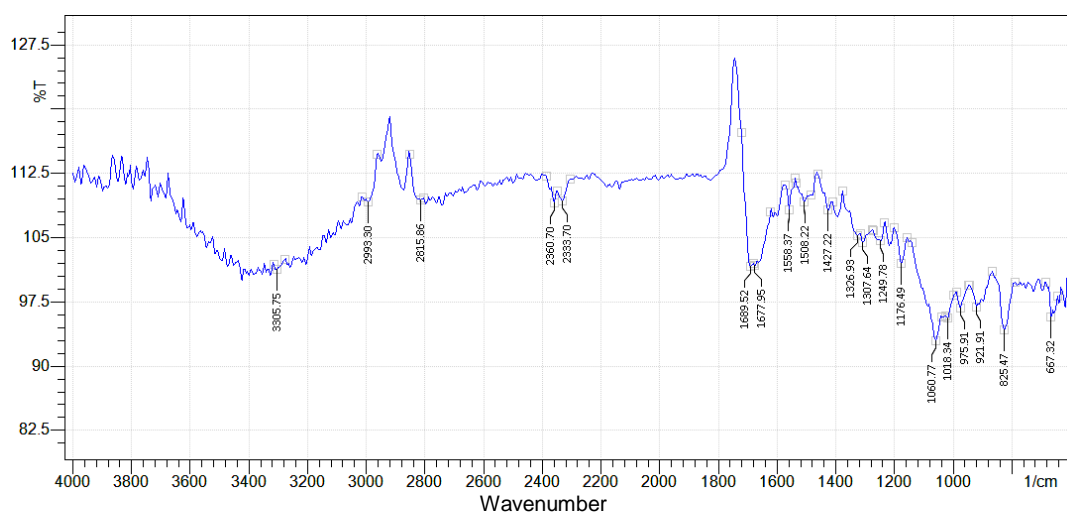
Figure 6. FTIR Spectra on Mn-N-TiO$_2$/Ti electrode

      The FTIR spectrum above indicated the specific regions which presence of molecular vibrations in Mn-N-TiO$_2$/Ti electrode. Figure 6 the absorption in 1558.37 cm^{-1} shows the vibrations of O-H and N-H. The uptake appears in 1427.22 cm^{-1} the presence of N-O bonding vibrations. Wavenumber of 3305.75 cm^{-1} shows the O-H stretching from H$_2$O molecule vibration trapped in Mn-N-TiO$_2$/Ti electrode [38]. According to Yang et al. absorptions that appear on wavenumber of 1249.78 cm^{-1} and 1176.49 cm^{-1} indicate the presence of Ti-N bonding vibrations [39]. While, absorptions at the wavenumber of 2330.70 cm^{-1} and 2360.70 cm^{-1} indicate the presence of Ti-O bond vibration [26]. Absorption below 1000 cm^{-1} indicates Mn-O bond [40]. The absorption at wavenumber of 1060.77 cm^{-1} the existence of manganese metal ion attached to electrode surface [26].

3.4. *Photocurrent Response by Amperometry (I-t)*

Photocurrent response measurements were conducted by using a potentiostat DY2100B with a Multi-Pulse Amperometry (MPA) technique at a bias potential of 500 mV. This condition to obtain the high-potential bias and photocurrent response. The range detection was arranged 1 s to obtain the photocurrent value every 1 s for 60 s of measurement time. It was expected the stability of data and minimized the possibility of electrode heat due to exposure of visible light. Photocurrent response was obtained when the potentiostat has turned on during 10 s in dark condition. This condition to obtain the data with uniformity of illumination time between photocurrent. After 10 s the visible lamp turned on exhibit the excited initial photocurrent due to separate of electron-hole and initiating a reduction-oxidation reaction.
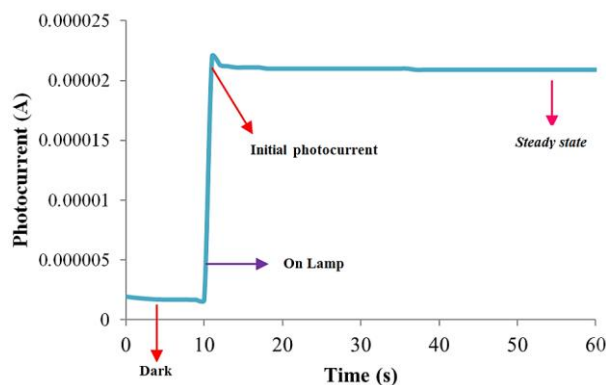
Figure 7. Photoelectrocatalysis profile using Mn-N-TiO$_2$/Ti in NaNO$_3$ 0.1M solution

Figure 7 shows the profile of photocurrent during measurement time ranges. Measurements with visible light off will result in background current which is the initial state of the solution. When the lights were switched on, there was a large current surge that indicated the occurrence of electron movement due to the reaction on surface of Mn-N-TiO$_2$/Ti electrode. The resulting current will decrease as the time of measurement increases, resulting in steady state. Steady state currents are formed because there is an equilibrium between the analytical fraction in surface of anode and diffusion of analyte from body of the solution [29,41].

4. Conclusion

We have studied the possibility of using the double doped i.e. Mn as metal and N as non-metal on the TiO$_2$/Ti hydrothermal electrode to be applied to COD sensor. The existence of N on TiO$_2$/Ti characterized by using FTIR showed the presented of Ti-O, Ti-N, N-O, and Mn-O bonds. Supported by SEM-EDX showed a thin layer formed of Mn and N on TiO$_2$/Ti surface with the spectrum of Mn, N, Ti, O at 0.277 KeV, 0.677 KeV, 4.508 KeV, and 0.579 KeV, respectively. The photoelectrochemical test using a potentiostat was indicated that Mn-N-TiO$_2$/Ti electrode active under visible light.

5. Acknowledgement

6. References

[1] Dzinun H, Othman M H D, Ismail A F, Puteh M H, Rahman M A, Jafar J 2015 *Chem. Engineer. J.* **269** 255.

[2] Maulidiyah, Ritonga H, Faiqoh C E, Wibowo D, Nurdin M 2015 *Biosci. Biotechnol. Res. Asia* **12** 1985.

[3] Zhang Q, Wang H, Fan X, Lv F, Chen S, Quan X 2016 *Surface & Coatings Technol*. **298** 45.

[4] Nurdin M 2014 *Int. J. Pharm. Bio Sci.* **5** 360.

[5] Maulidiyah, Ritonga H, Salamba R, Wibowo D, Nurdin M 2015 *Int. J. ChemTech Res.* **8** 645.

[6] Maulidiyah, Nurdin M, Erasmus, Wibowo D, Natsir M, Ritonga H, Watoni A H 2015 *Int. J. ChemTech Res.* **8** 416.

[7] Maulidiyah, Nurdin M, Widianingsih E, Azis T, Wibowo D 2015 *ARPN J. Eng. & Appl. Sci.* **10** 6250.

[8] Maulidiyah, Nurdin M, Wibowo D, Sani A 2015 *Int. J. Pharma. Pharmaceu. Sci.* **7** 141.

[9] Shirsath S R, Pinjari D V, Gogate P R, Sonawane S H, Pandit A B 2013. *Ultrasonics Sonochem.* **20** 277.

[10] Nurdin M, Muzakkar M Z, Maulidiyah M, Nurjannah M, Wibowo D 2016. *J. Mater Environ. Sci.* **7** 3334.

[11] Anitha B, Ravidhas C, Venkatesh R, Raj A M E, Ravichandran K, Subramanian B, Sanjeeviraja C 2017 *Phys. E:Low-dimensional Systems & Nanostruc.* **91** 148.

[12] Sacco O, Vaiano V, Han C, Sannino D, Dionysiou D D 2015 *Appl. Catal. B: Environ.* **164** 462.

[13] Maulidiyah, Wibowo D, Hikmawati, Salamba R, Nurdin M 2015 *Orient. J. Chem.* **31** 2337.

[14] Karamian E, Abdellahi M, Khandan A, Abdellah S 2016 *J. Alloys & Compounds* **679** 375.

[15] Yin W J, Chen S, Yang J H, Gong X G, Yan Y, Wei S H 2010 *Appl. Phys. Let.* **96**.

[16] Quan F, Hu Y, Zhang X, Wei C 2014 *Appl. Surface Sci.* **320** 120.

[17] Nurdin M, Maulidiyah, Watoni A H, Abdillah N, Wibowo D 2016 *Int. J. ChemTech Res.* **9** 483.

[18] Nurdin M, Zaeni A, Maulidiyah, Natsir M, Bampe A, Wibowo D 2016 *Orient. J. Chem.* **32** 2713.

[19] Gaikwad P N, Hankare P P, Wandre T M, Garadkar K M, Sasikala R 2016 *Materials Sci. & Eng.:B* **205** 40.

[20] Nurdin M, Ramadhan L O A N, Darmawati, Maulidiyah, Wibowo D 2017. *J. Coatings Technol. & Res.* DOI: 10.1007/s11998-017-9976-8

[21] Xin W, Zhu D, Liu G, Hua Y, Zhou W 2012 *Int. J. Photoenergy*, **1**.

[22] Ruslan, Mirzan M, Nurdin M, Wahab A W 2016 *Int. J. Appl. Chem.* **12** 399.

[23] Mahadik M A, Shinde S S, Hunge Y M, Mohite V S, Kumbhar S S, Moholkar A V, Rajpure K Y, Bhosale C H 2014 *J. Alloys & Compounds* **611** 446.

[24] Choudhury B, Paul S, Ahmed G A, Choudhury A 2015 *IOPScience* **2** 096.

[25] Hu Y, Zhang X, Wei C 2009 *Materials Sci. Forum* **620** 683.

[26] Zhao Y F, Li C, Lu S, Liu R X, Hu J Y, Gong Y Y, Niu L Y 2016 *J. Solid State Chem.* **235** 160.

[27] Yao N, Wang J, Zhou Y 2014 *Sensors*. **14** 9949.

[28] Wibowo D, Ruslan, Maulidiyah, Nurdin M 2017 *IOP Conference Series: Materials Science and Engineering* xx xx.

[29] Nurdin M, Wibowo D, Supriyono, Febrian M B, Surahman H, Krisnandi Y K, Gunlazuardi J 2009 *MAKARA SAINS*, **13(1)**: 1.

[30] Maulidiyah, Tribawono D S, Wibowo D, Nurdin M 2016 *Anal. Bioanal. Electrochem.* **8** 761.

[31] Nurdin M, Maulidiyah 2014 *Int. J. Sci. Technol. Res.* **3** 122.

[32] Sharma S, Chaudhary S, Kashyap S C, Sharma S K 2011 *Journal of Applied Physics* **109** 1.

[33] Xiong L-B, Li J-L, Yu Y 2012 *J. Nanomaterials* **2012** 1.

[34] Purnama A, Priatmoko S, Wahyuni S 2013 *Indonesian J. Chem. Sci.* **2** 200.

[35] Hikmawati, Watoni A H, Wibowo D, Maulidiyah, Nurdin M 2017 *IOP Conference Series: Materials Science and Engineering* xx xx.

[36] Zhao K, Wu Z, Tang R, Jiang Y 2013 *J. the Korean Chemical Soc.* **57** 176.

[37] Larios A P, Lartundo L, Mantilla A, Gordillo A H 2016 *Catal. Today* **266** 9.

[38] Qian J, Cui G, Jing M, Wang Y, Zhang M, Yang J 2012 *Int. J. Photoenergy* **1**.

[39] Yang G, Jiang Z, Shi H, Xiao T, Yan Z 2010 *J. Materials Chem.* **20** 5301.

[40] Xin W, Zhu D, Liu G, Hua Y, Zhou W 2012 *Int. J. Photoenergy* **1**.

[41] Arham Z, Nurdin M, Buchari B 2016 *Int. J. ChemTech Res.,* **9** 113.